A Model for the Initiation of Hydrogen Embrittlement Cracking at Notches in Gaseous Hydrogen Environments

P. DOIG AND G. T. JONES

A model for the initiation of hydrogen embrittlement cracking in gaseous hydrogen environments is presented. The model is based on the stress-induced diffusion of hydrogen atoms to the regions of high triaxial stress ahead of a plastically strained notch. The influence of yield stress and notch geometry on the apparent threshold stress intensity for embrittlement are considered and derived analytically. The time dependence for crack initiation for apparent stress intensities above the threshold is derived from a simple diffusion model. The results of the model are in agreement with reported hydrogen embrittlement phenomena.

1. INTRODUCTION

THE deleterious effect of hydrogen on the mechanical properties of high strength steels is a well-known phenomenon in the area of environment sensitive mechanical behavior of materials. The phenomenon is commonly termed 'hydrogen embrittlement' and has long been encountered in a range of processes which involve the production of hydrogen such as steelmaking,[1] welding,[2] electroplating[3] and corrosion.[4] More recently, however, hydrogen embrittlement has been observed to occur in high strength steels in gaseous hydrogen atmospheres over a wide range of pressure (down to less than 100 Pa) and temperature.[5,6] This has recently been highlighted by the failure of a rotor end-ring in hydrogen cooled alternator at Nanticoke, Canada,[7] and is of interest because of the wide-spread use of hydrogen cooling of generators in the electrical power supply industry.

There have been a number of theories proposed to explain the observed embrittling effect of hydrogen, most of which, however, are really based on the original proposals of Troiano and coworkers.[8,9] These investigators put forward the concept of a long range diffusion of hydrogen to the triaxial stress field developed ahead of a stressed notch or crack. Since then, this concept has been extended to include failure mechanisms based on void formation[10] by hydrogen precipitation, reduction of the cohesive strength of the metal-metal bond[9,11] and surface energy considerations involving a lowering of the Griffiths fracture energy[12,13] by adsorption of hydrogen. Whatever the detail of these various models they all require the development of a critical concentration of hydrogen and, according to Troiano,[9] this concentration is developed by the stress induced segregation of hydrogen to the regions of high triaxial stress.

Studies carried out on hydrogen-induced failure of notched high strength steel specimens indicate that an incubation time precedes cracking.[9,14] Cracking then takes place discontinuously at a slow rate until a critical stress intensity κ_{IC} is attained and rapid failure occurs. A lower critical stress intensity κ_{TH} exists below which delayed failure is not observed. This lower stress intensity increases with decreasing material yield stress until the phenomenon of delayed failure is eliminated. The essential characteristics of the delayed failure are shown schematically in Fig. 1.

The purpose of the present work is to develop a model for the development of hydrogen cracking at notches in a gaseous hydrogen environment.

2. MODEL FOR THE INCUBATION OF HYDROGEN INDUCED CRACKING

2.1 Stress Considerations

The interaction, U, controlling solute segregation in a stress field is given by:[15]

$$U = p\,\Delta V \qquad [1]$$

where p is the pressure tensor of the stress field and ΔV is the change in atomic volume due to the insertion of a solute atom. This leads to a solute concentration build up, C_x, at any point, x, within the stress field given by:[16]

$$C_x = C_0 \exp\left[\frac{p\,\Delta V}{kT}\right] \qquad [2]$$

where C_0 is the equilibrium concentration in the absence of stress,* k is Boltzmann's constant and T is the absolute temperature. This may be given as:[17]

$$C_x = C_0 \exp\left[\frac{\sigma_i V_H}{3RT}\right] \qquad [3]$$

where V_H is the partial molar volume, R is the gas constant, (= kN where N is the Avogadro number), σ_i is the summation of the principal stresses such that $\sigma_i/3$ is the hydrostatic component of the applied stresses.

The hydrostatic stress distribution ahead of a notch in plane strain is shown schematically in Fig. 2. For plane strain and assuming a perfectly elastic-plastic solid with no work hardening, we may use Hill's[19] slip-line field equation for the hydrostatic stress in

*Sievert's law states that the value of C_0 is related to the external gas pressure from the dissociation reaction $H_2 \rightarrow 2H$ such that $C_0 \propto (\text{pressure})^{1/2}$ [18]

P. DOIG and G. T. JONES are Research Officers, Central Electricity Generating Board, South East Region Scientific Services Department, Gravesend, Kent, UK.

Manuscript submitted February 24, 1977.

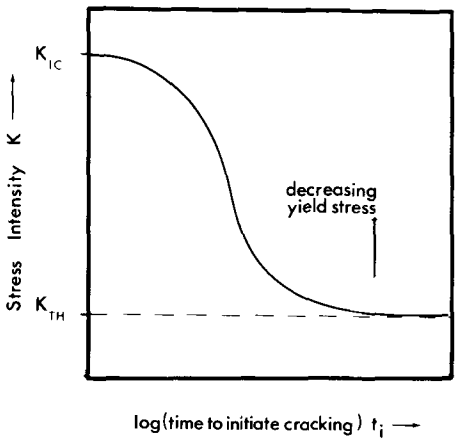

Fig. 1—Schematic diagram showing time to the initiation of hydrogen induced cracking as a function of stress intensity.

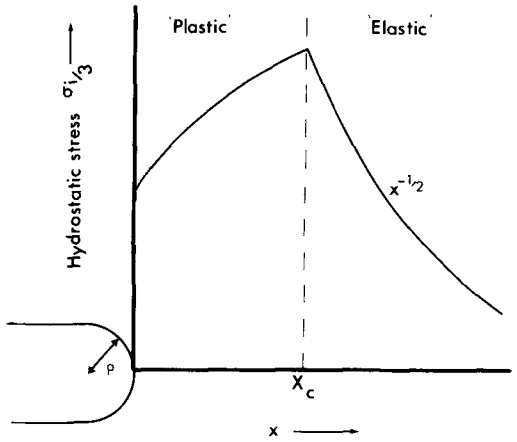

Fig. 2—Schematic diagram showing the distribution of hydrostatic stress ahead of a plastically deformed notch.

the "plastic zone" immediately ahead of a notch of radius ρ given by:[20]

$$\frac{\sigma_i}{3} = \sigma_y \left[\ln \left(1 + \frac{\chi}{\rho} \right)^{+1/2} \right] \qquad [4]$$

where σ_y is the material's yield strength and χ is the distance ahead of the notch.

For sharp notches where $\rho \ll a$ (the notch depth), the distribution of hydrostatic stress in the "elastic regime" may be assumed, for simplicity, to be given by the solution for a sharp crack, [21] *i.e*:

$$\frac{\sigma_i}{3} = 2/3\,(1 + \nu) \cdot \frac{\kappa_A}{(2\pi\chi)^{1/2}} \qquad [5]$$

where ν is Poisson's ratio and κ_A is the apparent applied stress intensity. This assumption neglects the effect of the redistribution of notch tip stresses due to plasticity and is therefore approximately correct only for plastic zone sizes that are small in relation to other physical dimensions.

For cracks we may use similar equations with the radius ρ replaced by an effective ρ^+ equal to half the crack opening displacement:[22]

$$\rho^+ = \kappa^2/2\sigma_y E. \qquad [6]$$

The position of maximum hydrostatic stress χ_c, in Fig. 2, is derived by combining Eqs. [4] and [5].

In reality, stress redistribution and work hardening will affect these stress profiles. Comparison with available finite element analyses for sharp notches and cracks, however, suggests that these equations will give approximations that are near enough to the real profiles for the present purpose.

From Eqs. [3], [4] and [5] the equilibrium concentration profiles for hydrogen in the two regimes are given by:

$$\text{"plastic"}\ C_\chi = C_0 \exp\left[\frac{\sigma_y V_H}{RT} \{\ln(1 + \chi/\rho) + 1/2\} \right] \qquad [7]$$

$$\text{"elastic"}\ C_\chi = C_0 \exp\left[\frac{\kappa_A V_H}{RT} \cdot \frac{2(1+\nu)}{3(2\pi\chi)^{1/2}} \right]. \qquad [8]$$

The equilibrium concentration of hydrogen at the root of the notch when $\chi = 0$ is given from Eq. [7]:

$$C_{\chi=0} = C_0 \exp\left[\frac{\sigma_y V_H}{2RT} \right]. \qquad [9]$$

2.2 Diffusion Considerations

Upon loading a notched or cracked specimen, with an initial zero concentration of hydrogen, in an atmosphere of H_2 gas, hydrogen molecules dissociate at the strained root according to:

$$H_2 \rightleftarrows 2H^{\cdot}$$

and the resulting hydrogen atoms diffuse into the metal towards the region of highest hydrostatic stress.

We may simplify the diffusion problem and solve analytically for the local hydrogen build-up by assuming a plane infinite source of hydrogen diffusing into a

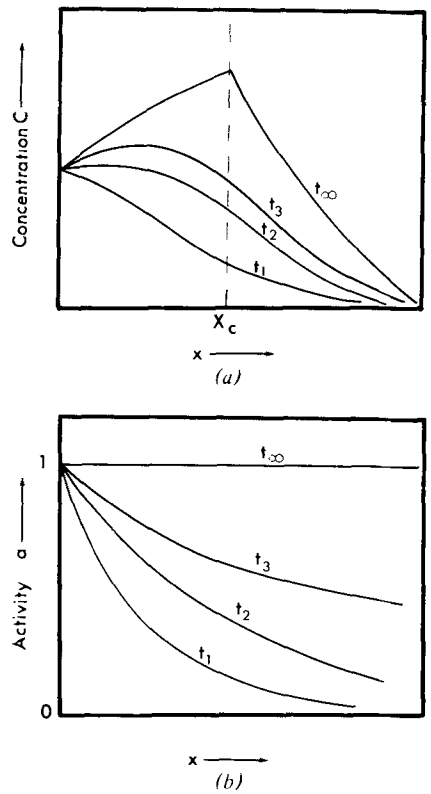

Fig. 3—Schematic diagrams showing the distribution of concentration (*a*) and activity (*b*) as a function of position, χ, ahead of a notch and time $t_1 < t_2 < t_3 < t_\infty$.

plane infinite specimen with a fixed concentration, $C_{\chi=0}$, at the interface and by considering the "activity", $\alpha_{\chi,t}$, at any point (χ) and time (t) where:

$$\alpha_{\chi,t} = \frac{C_{\chi,t}}{C_{\chi,t_\infty}}. \quad [10]$$

The solution for the activity in terms of χ and t (Ref. 23) is:

$$\alpha_{\chi,t} = 1 - erf\left[\frac{\chi}{2(Dt)^{1/2}}\right] \quad [11]$$

where D is the diffusion coefficient of hydrogen in metal and:

$$erf\, z = 2/\pi^{1/2} \int_0^z \exp(-y^2)dy. \quad [12]$$

This assumes that D is independent of stress and concentration, which has been verified for hydrogen in iron over a range of stress by Beck and coworkers[24] using very high sensitivity electrochemical permeation techniques. The activity, therefore, is unity at $t = \infty$ when the concentration becomes the equilibrium concentration C_χ ($= C_{\chi,t_\infty}$) as determined by the stress profile. For times $t_1 < t_2 < t_3 < t_\infty$ the concentration or activity profiles take the form as shown schematically in Figs. 3(*a*) and (*b*).

3. THE CRITERION FOR HYDROGEN INDUCED CRACK INITIATION

It is usual in notch fracture mechanics studies to accept that for crack initiation it is not only necessary to achieve a critical stress or strain level for fracture but that it must also be achieved over a distance appropriate to the micromechanism involved (*e.g.* in their hydrogen induced crack propagation model Gerberich *et al*[25] assumed the controlling length parameter to be the grain size). In the present model we assume that for crack initiation a critical hydrogen concentration level, C_c, must be achieved over an unspecified distance, d_c, determined by the microstructure.

The threshold apparent stress intensity, κ_{ATH}, for any particular notch geometry (including cracks) as depicted in Fig. 1 is interpreted as being that apparent stress intensity that just allows the C_c to be achieved over the distance d_c at $t = \infty$, *i.e.*, when $\alpha_{\chi,t} = 1$. If σ_c is the critical hydrostatic stress associated with C_c then the critical distance d_c is given by:

$$d_c = \frac{1}{2\pi}\left[\frac{2(1+\nu)\kappa_{ATH}}{3\sigma_c}\right]^2 - \rho\left[\exp\left\{\frac{\sigma_c}{\sigma_y} - \frac{1}{2}\right\} - 1\right] \quad [13]$$

and in theory two experimental values for κ_{ATH} for different values of ρ are sufficient to determine d_c and σ_c.

For "mild" notches ($d_c \ll \rho$) the rate of change of stress in the peak stress region will in reality be low compared with the rate of change for cracks and very sharp notches. For "mild" notches therefore, the peak stresses are likely to predominate over distances that are large compared with d_c and the controlling parameter becomes simply the critical stress σ_c, *i.e.*:

$$\kappa_{ATH} = \frac{3\sigma_c}{2(1+\nu)}\left[2\pi\rho\left(\exp\left\{\frac{\sigma_c}{\sigma_y} - \frac{1}{2}\right\} - 1\right)\right]^{1/2}. \quad [14]$$

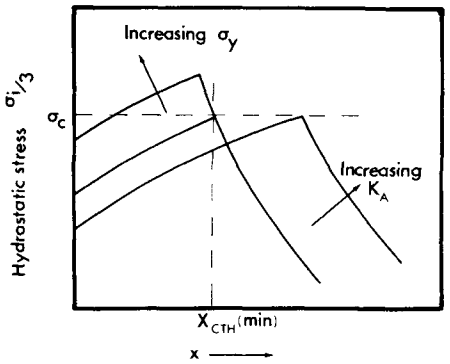

Fig. 4—Schematic diagram showing the influence of σ_y and κ_A on the hydrostatic stress ahead of a notch.

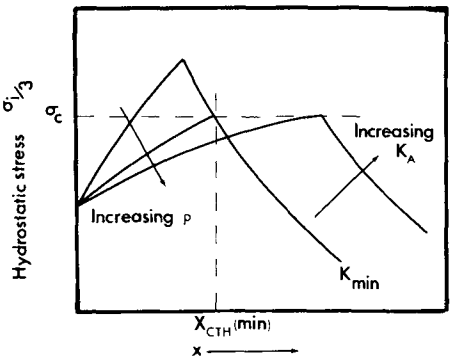

Fig. 5—Schematic diagram showing the influence of notch root radius, ρ, on the hydrostatic stress ahead of a notch.

3.1 The Influence of Yield Stress and Notch Root Radius on κ_{ATH}

Equation [14] suggests that if σ_c remains constant, κ_{ATH}, for a given notch root radius, decreases with increasing σ_y, as shown schematically in Fig. 4 ($d\kappa_{ATH}/d\sigma_y$ is always $-ve$ and $d^2\kappa_{ATH}/d\sigma_{y^2}$ is $+ve$). This model also suggests that there may be a lower limit to κ_{ATH} that would make it constant at higher σ_y values. This limit (again, assuming that σ_c is independent of σ_y) is achieved when $\sigma_y = 2\sigma_c$.

The influence of notch root radius on the hydrostatic stress distribution is shown schematically in Fig. 5. For constant σ_y and σ_c Eq. [14] suggests that for mild notches κ_{ATH} will be proportional to $\rho^{1/2}$, and for sharp notches where the combined effects of the opening displacement and the critical distance, d_c, limitation predominate, κ_{ATH} will approach a minimum.

3.2 The Influence of $\kappa_A > \kappa_{ATH}$ on Time to Initiate Cracking, t_i

The time to initiate cracking is assumed to be the time required to build up a critical hydrogen concentration, C_c, or a critical activity, α_c, over the critical distance, d_c. For mild notches we may again neglect d_c and assume that initiation will occur if C_c or α_c is reached anywhere in the notch tip region. From the foregoing analysis however the minimum critical activity is always at χ_c and it follows from the form of the diffusion equation that the critical activity is first reached at χ_c. The time to initiation, t_i, is therefore obtained from:

$$1 - erf\left\{\frac{\chi_c}{2(Dt_i)^{1/2}}\right\} = \exp\left\{\frac{V_H}{RT}\left[\sigma_c - \frac{\sigma_i\chi_c}{3}\right]\right\} \quad [15]$$

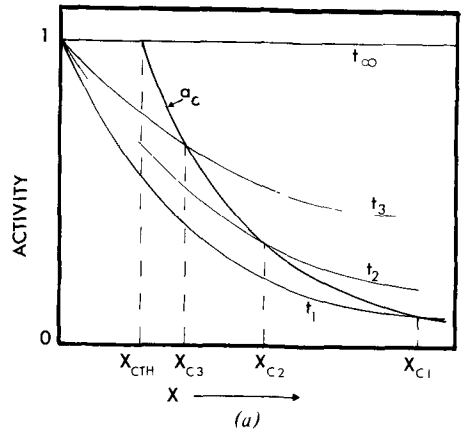

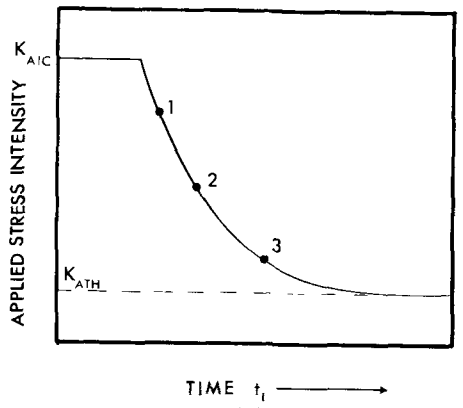

Fig. 6—Schematic diagrams showing: (*a*) the time required for the critical activity to be obtained as a function of peak stress position (χ_c)—related to κ_A; (*b*) resulting time to initiate cracking as a function of κ_A, for $t_1 < t_2 < t_3 < t_\infty$.

where σ_c is obtained from κ_{ATH} and Eq. [14], and $\sigma_i/3$ (at χ_c) from Eq. [4]. This may also be written as:

$$1 - erf\left\{\frac{\chi_c}{2(Dt_i)^{1/2}}\right\} = \exp\left\{\frac{\sigma_y V_H}{RT}\left[\ln\left\{\frac{\rho + \chi_{cTH}}{\rho + \chi_c}\right\}\right]\right\} \quad [16]$$

where χ_{cTH} is the critical distance at threshold given by:

$$\sigma_y\left[\ln\left\{1 + \frac{\chi_{cTH}}{\rho}\right\} + \frac{1}{2}\right] = \frac{2}{3}(1+\nu)\cdot\frac{\kappa_{ATH}}{(2\pi\chi_{cTH})^{1/2}}. \quad [17]$$

The implications of these equations are shown schematically in Figs. 6(*a*) and (*b*). The critical activity, α_c, is shown in Fig. 6(*a*) as a function of χ_c. Equation [11] has been used to superimpose the activity levels as a function of time ($t_1 < t_2 < t_3$) and distance χ. As χ_c increases ($\chi_{c1} > \chi_{c2} > \chi_{c3}$) for increasing κ_A so the time to initiate cracking, t_i, decreases as shown in Fig. 6(*b*).

4. COMPARISON WITH EXPERIMENTAL DATA

Little experimental data on crack initiation from notches in gaseous hydrogen is available at present. However, recently obtained data points for an austenitic steel tested in hydrogen at 400 kPa pressure and 298 K using notched $C\kappa$ specimens with a notch root radius of 0.8×10^{-3} m, suggest that the model is capable of predicting realistic times for crack initiation. Figure 7 shows the data points obtained and the results that would be expected using Eqs. [16] and [17]

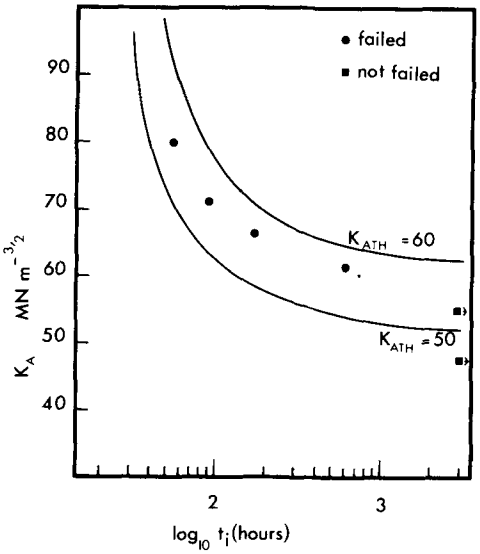

Fig. 7—Experimental data points for an austenitic steel shown in comparison with the failure times predicted by the model for two κ_{ATH} values using Eqs. [16] and [17].

for κ_{ATH} values of 50 and 60 $MNm^{-3/2}$ and the following properties:

σ_y = 1000 MNm^{-2}
V_H = 3×10^{-6} $moles^{-1}$ m^3 (Ref. 26)
RT = 2500 NM $mole^{-1}$
D = 10^{-11} m^2 s^{-1} (Ref. 13).

For this material and specimen geometry, the measured apparent fracture toughness, κ_{AIC}, in air at 298 K was 120 $MNm^{-3/2}$. The calculated curves are qualitatively similar to those shown in Fig. 1. The curve is very sensitive to values of κ_{ATH}, V_H and ρ and is displaced to longer times with increasing values of κ_{ATH} and ρ and decreasing values of V_H.

5. DISCUSSION

The above model for the time dependent initiation of hydrogen embrittlement is based on the assumption that the rate controlling step is the bulk diffusion of hydrogen within the metal lattice. Other possible rate controlling processes include a) the dissociation of hydrogen gas molecules into hydrogen atoms at the strained notch surface, b) the inhibiting effect of surface oxide films on the transport of hydrogen atoms to the metal surface and c) the actual nucleation of the hydrogen embrittlement crack by whatever mechanism may be operating (see Section 1).

a) Results obtained from deuterium gas permeation experiments in austenitic steels have shown the activation energy controlling the permeation rate is given by the sum of the energies describing the diffusion and solubility only.[27] Consequently, the flux of deuterium into the metal is controlled by the solubility and diffusion of the deuterium within the metal and the dissociation into atoms does not contribute to the overall rate. Therefore, it is reasonable to conclude that the dissociation kinetics of hydrogen will not be rate determining in the overall hydrogen embrittlement process.

b) Several workers[27-31] have demonstrated the inhibiting effect of oxide films on the permeation of hydrogen into a variety of steels. Reductions in perme-

ability of up to one thousandfold have been reported.[28] However, for specimens which are plastically strained in pure hydrogen, the oxide films will be ruptured after very small plastic strains. Consequently, bare metal surfaces are exposed and the above diffusion model for the kinetics of hydrogen embrittlement will apply. Where surface oxide films can reform, for example, with oxygen contaminent in the hydrogen, the permeation kinetics of the hydrogen through the oxide films may contribute to the overall rate controlling process.

The equation describing the diffusion of hydrogen into an oxide covered metal has been given by Crank[23] as:

$$\alpha_2 = \frac{2k}{1+k}\sum_{n=0}^{\infty}\mu^n\left[1 - erf\left[\frac{(2n+1)L + kx}{2(D_1 t)^{1/2}}\right]\right]$$

where $k = \left[\frac{D_1}{D_2}\right]^{1/2}$ and $\mu = \left[\frac{1-k}{1+k}\right]$, D_1 and D_2 are the diffusion coefficients of hydrogen in the oxide film and metal respectively, α_2 is the activity of hydrogen and L is the oxide film thickness. The resulting activity profiles for hydrogen in the oxide film/metal couple are shown schematically for different times, (Fig. 8), $t_1 < t_2$ and $D_1 \ll D_2$ and $\alpha_2 \ll \alpha_{x,t}$ (from Eq. [11]) for fixed values of x and t.) Consequently, the time to achieve the critical activity for crack initiation, α_c, will increase depending on D_1 and L. There are at present, no accurate data available for D_1 values in surface oxides but only empirical observations that in general $D_1 \ll D_2$. Therefore, even very thin continuous oxide films will have a large effect on the time to initiate an hydrogen embrittlement crack.

c) The observation that the incubation of hydrogen embrittlement cracking in precharged steel specimens occurs very rapidly ($\leq 10^3$s)[9,14] and that the kinetics of incubation rate follow an activation energy equal to that describing the diffusion of hydrogen in the steel,[14] suggest that any rate effects associated with the crack initiation mechanism are not controlling the overall cracking process and that the rate controlling step is the bulk diffusion of hydrogen in the steel.

The stress distributions described in the above model for hydrogen embrittlement are derived for a perfectly elastic-plastic solid with zero work-hardening, and the diffusion solutions employed in this analysis do not take into account the actual shape of the stress field ahead of the notch. A more accurate solution of the stress distribution requires the use of finite element computer methods.

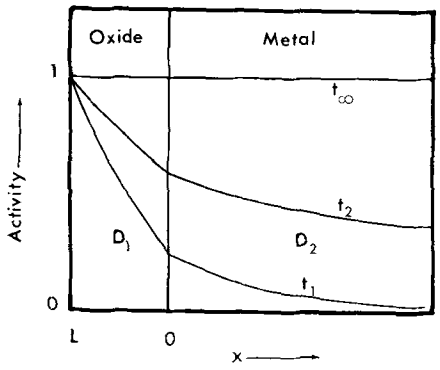

Fig. 8—Schematic diagram of the activity profiles of hydrogen in an oxide covered metal for times $t_1 < t_2 < t_\infty$ where diffusion coefficient $D_1 \ll D_2$.

It has been proposed[32-35] that large amounts of cold work can influence both the diffusion and solubility behavior of hydrogen in iron. Such proposals are based on the influence of dislocations providing both easy diffusion paths, *i.e.* lower activation energy, and preferential lattice sites for hydrogen atoms in solution. Most data, however, used permeability as the variable and the separate influences diffusivity and solubility are not apparent. Thermodynamic calculations, however, based on the strain energy associated with the dislocation[15,26] have shown that the average solubility of hydrogen in a heavily cold worked lattice can be ~100 times that in an annealed structure. Such an effect will change the average equilibrium hydrogen concentration ahead of the plastically deformed notch but will not affect the stress induced matrix concentration which is controlling.

This work presents a model for the initiation of hydrogen embrittlement cracking which includes a bulk diffusion controlled hydrogen build-up as the rate controlling step, together with the concept of a critical hydrostatic stress, σ_c, a related critical hydrogen concentration, C_c, a critical minimum distance, d_c, and the thermodynamic variable, V_H, the partial molar volume. It is readily apparent from this model that the critical hydrostatic stress is reached much sooner under conditions of plane strain rather than plane stress. Consequently, the hydrogen embrittlement behavior will be strongly dependent on the stress distribution and will occur more readily in thicker sections where the hydrostatic stress component is greater. The critical distance, d_c, is related to the microstructural feature associated with the initiation of cracking. We may, therefore, conclude that susceptibility to embrittlement will be strongly influenced by microstructure.

6. CONCLUSIONS

A quantitative model for hydrogen embrittlement at notches in steels in gaseous hydrogen environments is proposed which predicts:

1) A decrease in the threshold apparent stress intensity for embrittlement, κ_{ATH}, with increasing yield stress σ_y.

2) A lower limit to κ_{ATH} with increasing σ_y, which is determined by a microstructurally controlled length parameter.

3) An increase in κ_{ATH} with increasing notch root radius.

4) A lower limit to κ_{ATH} with decreasing ρ determined by the length parameter, d_c.

5) An infinite time for embrittlement for applied apparent stress intensity $\kappa_A = \kappa_{ATH}$.

6) A decreasing time for failure for $\kappa_A > \kappa_{ATH}$.

Initial indications are that the model is capable of predicting failure times that are consistent with experimental data.

ACKNOWLEDGMENTS

The authors wish to thank Dr. P. E. J. Flewitt for useful discussions. This paper is published by permission of the Director General, South Eastern Region, Central Electricity Generating Board.

REFERENCES

1. J. H. Andres, H. Lee, A. K. Millik, and A. G. Quarrell *J. Iron Steel Inst.*, 1946, vol. 153, p. 67.
2. C. R. Tottle and H. C. Wright: *The Metallurgy of Welding, Brazing and Soldering,* p. 56, American Elsevier, New York, N. Y., 1960.
3. R. H. Raring and J. A. Rinebolt: *Trans. ASM,* 1956, vol. 48, p. 198.
4. R. Broom and A. J. Nicholson: *J. Inst. Metals,* 1960, vol. 89, p. 183.
5. R. A. Oriani and P. H. Josephic: *Acta Met.*, 1974, vol. 22, p. 1065.
6. G. G. Hancock and H. H. Johnson: *Trans. TMS–AIME,* 1966, vol. 236, p. 513.
7. C. B. Jolly and M. C. Murphy: Paper presented at the 1975 Fall Meeting of the Thermal and Nuclear Power Section of the Canadian Electrical Association, Halifax, Nova Scotia, October, 1975.
8. E. A. Steigerwald, F. W. Schaller, and A. R. Troiano. *Trans. TMS–AIME,* 1959, vol. 215, p. 1048.
9. A. R. Troiano: *Trans. ASM,* 1960, vol. 52, p. 54.
10. A. S. Tetelman: *Fracture of Solids,* p. 671, John Wiley and Sons, New York, N. Y., 1962.
11. J. G. Mortlett, H. H. Johnson, and A. R. Troiano: *J. Iron Steel Inst.*, 1958, vol. 189, p. 37.
12. N. J. Petch: *Phil. Mag.*, 1956, vol. 1, p. 331.
13. D. P. Williams and H. G. Nelson: *Met. Trans.*, 1970, vol. 1, p. 63.
14. C. F. Barth and E. A. Steigerwald *Met. Trans.*, 1970, vol. 1, p. 3451.
15. A. H. Cottrell: *Dislocations and Plastic Flow in Crystals,* Clarendon Press, Oxford, 1953.
16. R. A. Oriani. *Fundamental Aspects of Stress Corrosion Cracking,* p. 32, NACE, Houston, USA, 1969.
17. W. W Gerberich and Y. T Chen, *Met. Trans. A,* 1975, vol. 6A, p. 27.
18. A. Sieverts: *Z. Metallk.*, 1929, vol. 21, p. 37.
19. R. Hill: *Mathematical Theory of Plasticity,* p. 248, Clarendon Press, Oxford, 1950.
20. A. J Wang *Quart. Appl. Mech.*, 1954, vol. 11, p. 427.
21. R. O. Ritchie, B. Francis, and W. L. Server: *Quart. Appl. Mech.*, 1976, vol. 7, p. 831.
22. J. F. Knott. *J. Strain Anal.*, 1975, vol. 10, p. 201.
23. J. Crank: *The Mathematics of Diffusion,* Clarendon Press, Oxford, 1970.
24. W. Beck, J. O. M. Bockris, J. McBreen, and L. Nanis: *Proc. Roy. Soc.*, 1965, vol. A290, p. 220.
25. W. W. Gerberich, Y. T. Chen, and C. St. John: *Met. Trans. A,* 1975, vol. 6A, p. 1485.
26. W. Beck, P. K. Subramanyan, and F. S. Williams. *Corrosion,* 1971, vol. 27, p. 115.
27. M. R. Louthan and R. G. Derrick. *Corros. Sci.*, 1975, vol. 15, p. 565.
28. C. L. Huffman and J. M. Williams: *Corrosion,* 1960, vol. 16, p. 430.
29. Yu. I Belyakov, Yu. I. Zvezdin, and A. A. Kurdyumov: *Fiz. Khin. Mekham Mater.*, 1970, vol. 6, p. 37.
30. J. C. Sherlock and L. L. Shreir: *Corros. Sci.*, 1970, vol 10, p. 561.
31. J. C. Sherlock and L. L. Shreir: *Corros. Sci.*, 1971, vol. 11, p. 543.
32. D. I. Phalen and D. A. Vaughan: *Corrosion,* 1968, vol. 24, p. 243.
33. C. M. Hudgins *Corrosion,* 1969, vol. 25, p. 116.
34. W. Beck: *Corrosion,* 1970, vol. 26, p. 86.
35. F. de Kazinczy: *Jernkont. Ann.*, 1955, vol. 139, p. 885.